



# Amorphous/nanocrystalline composites analysed by the Rietveld method

M. Baricco<sup>a,\*</sup>, S. Enzo<sup>b</sup>, T.A. Baser<sup>a</sup>, M. Satta<sup>a</sup>, G. Vaughan<sup>c</sup>, A.R. Yavari<sup>d</sup>

<sup>a</sup> Dipartimento di Chimica IFM and NIS/INSTM/CNISM, Università di Torino, Via, P. Giuria 9, 10125 Torino, Italy

<sup>b</sup> Dipartimento di Chimica, Università di Sassari, via Vienna 2, 07100 Sassari, Italy

<sup>c</sup> European Synchrotron Radiation Facility, E.S.R.F., B. P. 220, F - 38043, Grenoble, Cedex, France

<sup>d</sup> Laboratoire de Thermodynamique et Physico-chimie Metallurgique (LTPCM-UMR, 5614), Institut National Polytechnique de Grenoble, CNRS, 38402, Grenoble, France

## ARTICLE INFO

### Article history:

Received 10 July 2008

Received in revised form 29 October 2009

Accepted 4 November 2009

Available online 12 November 2009

### Keywords:

Amorphous materials

Rapid-solidification

Quenching

Crystal structure

X-ray diffraction

## ABSTRACT

The Rietveld refinement approach has been applied to semi-crystalline materials in the case of bulk metallic glasses. Specifically, the crystallisation behaviour of a  $\text{Fe}_{48}\text{Cr}_{15}\text{Mo}_{14}\text{Y}_2\text{C}_{15}\text{B}_6$  bulk metallic glass has been investigated by *in situ* X-ray diffraction obtained using a high intensity monochromatic synchrotron beam at the ID11 line of ESRF in Grenoble, France. From the Rietveld analysis of diffraction patterns, adapted to include a paracrystal model for describing the amorphous metal component, volume fraction of evolving phases, structure and microstructure parameters of nucleated phases have been followed as a function of run number, which turns out to be related to the applied temperature. Capabilities and limitations of the approach are discussed in terms of structural information.

© 2009 Elsevier B.V. All rights reserved.

## 1. Introduction

Dealing with single phase amorphous materials, the radial distribution function obtained by inversion of the total structure factor was used several times to point out similarities and differences existing between the atomic short range order in glassy structures and in crystals. This intuitive approach was largely used firstly for silicate glasses [1] and also for metallic glasses [2]. In this context, it appears worth of note the investigation by Sietsma and Thijssse [3] making reference to the “paracrystallinity” approach, originally proposed by Hosemann and Bagchi [4], in order to ascertain for the best models able to describe an amorphous metal structure, with highly distorted lattice, that exhibits only very broadened peaks. In this approach, assuming the existence of a “pseudo” unit cell, a pseudo-crystalline structure condition (at micro- or nano-scale) was considered, in the sense that the sequence of maxima in the diffraction pattern should be indexed by integers  $hkl$ , according to at least one of the crystallographic space groups. What makes “pseudo” the crystalline nature is the abnormal amount of lattice strain (ca 2.0%) and extremely reduced coherent diffraction domain size (1–2 nm). Of course, this approach turns out to be of reduced validity for a full description of the properties of an amorphous substance.

Concerning the opposite case of completely crystalline powdered mixtures, the structure properties may be successfully studied and precisely refined using the well established Rietveld method [5]. The Rietveld approach may in principle account for the structure of amorphous samples, though roughly, once the user is able to supply a reasonable and flexible “pseudo-crystalline” structure factor. In the case of amorphous silica, Le Bail [6] started from the  $\text{P}2_12_12_1$  crystalline structure factor of  $\text{SiO}_2$  in a Rietveld refinement and reported the modified structure and microstructure parameters which gave a satisfactory agreement between calculated and experimental X-ray and/or neutron diffraction patterns. Le Bail eventually used the refined atomic positions of cristobalite pseudo unit cell as input parameters for a reverse Monte Carlo approach to go beyond the intrinsic limits of this empirical and preliminary procedure. The limits of such “paracrystalline” results were discussed in comparison with the reverse Monte Carlo technique [7].

On the other hand, dealing with diffraction patterns of amorphous/crystal mixtures, so-called semi-crystalline systems, the Rietveld method is instinctively judged improper. As a matter of facts, alternative approaches were followed in the literature. In the case of semi-crystalline materials, Ruland [8] developed the X-ray diffraction (XRD) equations of the method for evaluating the amount of crystalline phases in an otherwise amorphous matrix. Integrating the volume of substance over the whole of reciprocal space and after suitable normalisation and extrapolation, a crystallinity factor ( $\chi_{\text{cr}}$ ) was defined as the amount of integrated intensities of crystalline phases with respect to the integrated

\* Corresponding author. Tel.: +39 011 670 7569; fax: +39 011 670 7855.

E-mail address: [marcello.baricco@unito.it](mailto:marcello.baricco@unito.it) (M. Baricco).

intensities from amorphous plus crystalline phases. It is clear that in order to determine the amorphous fraction  $x_{\text{am}} = 1 - x_{\text{cr}}$ , the most critical step lies in the separation of the amorphous scattering from that due to crystalline phases. Riello et al. [9] proposed a solution to the problem of accounting for the scattering of semi-crystalline materials in the Rietveld analysis by including the normalized scattering profile of an amorphous phase for which the chemical composition and density or the global sample composition was known. We should mention that essentially another line of work has been proposed within the Rietveld context to properly address the study of semi-crystalline systems making use of an internal standard. The method determines the amorphous fraction by difference between the measured and expected value of the standard fraction [10]. Conversely, the method that we are going to present here does not require any standard but attempts to model the amorphous scattering in an empiric and acceptable fashion “compatible” with the crystallographic rules of the Rietveld method as it was done by Lutterotti et al. [11], which in turn is based on previous work by Le Bail [6]. After calibrating the procedure in samples with known quantity of amorphous  $\text{SiO}_2$  and crystalline  $\text{Al}_2\text{O}_3$ , a quantitative analysis of the phases in a semi-crystalline system was obtained, including the amorphous component and avoiding the use of any internal standard [12]. Although both approaches have their own merits, the limitations involved in the use of an external standard can be easily recognized since the procedure assumes that the scattering contribution of the amorphous component is a part of the background.

The performance of the Rietveld method according to Lutterotti et al. [11] appears to be realistic in as much as the atomic density of the amorphous “paracrystal” is not too different from the true value and/or from the crystalline counterpart. If this holds, then also the nearest neighbour interatomic distances may be regarded as a broad but realistic estimate. So, in principle, an analysis can be conducted on XRD patterns of fully and partially amorphous materials by Rietveld refinement using the paracrystal model, although the structure information may not be completely sensible from the physical point of view. The advantage of this approach is that, together with the evaluation of the amorphous fraction, useful structural and microstructural information can be obtained on the remaining crystalline phases with a whole powder pattern refinement in a one-step numerical procedure, which shows the agreement between model and experiment. With this approach, an essential requisite is that the powder diffraction data are collected appropriately in terms of signal-to-noise and background ratio, as it can be obtained with a synchrotron source in relatively short times, thus enabling to follow the kinetics details.

The aim of this work is the application of the paracrystal model with Rietveld assessment for the description of amorphous/crystalline mixed systems, using diffraction data obtained with a synchrotron radiation. This approach will be applied to a Fe-based bulk metallic glass (BMG).

## 2. Experimental

Alloy ingots, with nominal composition  $\text{Fe}_{48}\text{Cr}_{15}\text{Mo}_{14}\text{Y}_2\text{C}_{15}\text{B}_6$ , have been prepared by arc melting a mixture of high purity elements under a Ti-gettered argon atmosphere. Each ingot has been melted three times in order to obtain a good homogeneity. The synthesis of BMGs has been obtained using a wedge-shaped copper mould in Ar atmospheres. Compositions have been confirmed by scanning electron microscopy (SEM) equipped with a microanalysis energy dispersive spectroscopy (EDS).

The high flux high-energy monochromatic radiation on ID11 beam line of the European Synchrotron Radiation Facilities (ESRF) has been employed for *in situ* structural characterisation during suitable thermal treatments. The energy of the photons used corresponds to an X-ray wave-length ( $\lambda$ ) of 0.01549 nm. The quartz crucibles containing the BMG samples were inserted inside an induction coil, vertically placed between the incident beam and a two-dimensional detector. Each pattern was recorded and then stored-in, while the sample was continuously heated or cooled. Note that in some cases our graphs reports the logarithmic intensities

times the scattering vector  $Q = 4\pi \sin \theta / \lambda$  in order to emphasize the occurrence of weak peaks at wide angles in the crystalline components and to verify the signal-to-background ratio simultaneously. A low signal-to-background ratio is expected to produce a marked ascending trend in a  $\log(I \times Q)$  plot.

The structures of the phases (whether crystalline, semi-crystalline or amorphous) are used by the MAUD program [12] to evaluate numerically and sum each correspondent pattern until fitting of the experimental data after minimizing the weighted sum of squared differences at each point. The basics of this numerical process and relevant equations are given in [5]. Summarizing, under the general assumption of a normal distribution of residuals (i.e., the difference between square root of calculated and experimental data points), the program is able to supply, within a fair degree of confidence that in turn depends on the signal-to-noise and background ratios of the pattern, the quantitative analysis of the phases, their structural parameters such as unit cell dimensions, crystallographic position of atoms, as well as the microstructure parameters, like the average crystallite size, anisotropy and the average lattice microstrain. As stated in the introduction, the starting structure factor of an amorphous substance should be chosen as to properly consider the chemical composition of the glass and its density. If the chemical composition is determined separately or already known *a priori* – as it is our case – it can be inserted in the pseudo-unit cell and maintained fixed in the occupation of Wyckoff sites during the numerical refinement. Meanwhile, changes in the atomic density can be contemplated in the least square adjustment by allowing the unit cell volume to vary through its lattice parameters. Other structure parameters that can be adjusted to accomplish a satisfactory description of experimental amorphous structure factor are atomic fractional coordinates  $x_j$ ,  $y_j$  and  $z_j$ , atomic displacement parameter  $B_j$ . Of course, after the selection of a specific crystal geometry, fractional coordinates may vary only according to the space group symmetry. For the description of line broadening effects, the MAUD programme uses pseudo-Voigt functions and adjusts the peak shape on account of simultaneous effects due to the average coherent domain of diffraction ( $D$ ) and amount of lattice disorder ( $\varepsilon$ ). The latter is generally understood as the square root of the mean square deviation of atoms from the (hkl) plane actually considered and it may be related to the  $g$ -factor of a paracrystal, as reported by Hindeleh and Hosemann [13]. The programme considers also the asymmetric distortion of the line shapes ascribable to stacking faults phenomena.

## 3. Results

The *in situ* XRD patterns of  $\text{Fe}_{48}\text{Cr}_{15}\text{Mo}_{14}\text{Y}_2\text{C}_{15}\text{B}_6$  bulk metallic glass showed a good signal-to-noise ratio, while the signal-to-background ratio appears less satisfactory due to the impossibility of adopting a monochromator in the diffracted beam, which otherwise would inhibit the fast acquisition of diffraction data. The typical haloes of an amorphous phase were observed in the first patterns [14,15]. Several crystal structures should be attempted in order to identify the most suitable paracrystalline structure useful to describe the experimental data of a fully amorphous sample. Since one significant parameter of the system concentration is the metal-metalloid ratio, which holds 79/21 for the present specimen, we have examined the potential for “paracrystal” refinement of the amorphous intensity of two basic cells, namely monoclinic  $\text{Fe}_5\text{C}_2$  (S.G.  $C12/c1$ ) and orthorhombic  $\text{Fe}_3\text{C}$  (S.G.  $Pnma$ ) type crystal structures. The results of the fitting procedure are shown in Fig. 1. At parity of efforts, the latter space group led to the best agreement with the experimental data, confirming the early expectations by Sietsma and Thijsse [3]. It is worth noting the capability of a paracrystalline model to describe this metal-metalloid amorphous system, in spite of its inherent physical limitations that were thoroughly discussed by Le Bail [6]. Note that the bump at ca 2% is due to the amorphous quartz capillary and it has been accounted for by the same structure factor reported by Lutterotti et al. for amorphous silica [11]. Also note that the plot of Fig. 1 shows the baseline assumed as background, according to a parabolic expression. For the sake of comparison, the very bottom lines of Fig. 1 give the residuals i.e., the weighted difference between calculation and experiment. It is from these residuals that the goodness-of-fit (GOF) indices are defined under the assumption of their uniformity and normal distribution [5]. Since GOF numbers are blind to a certain extent, the non-uniformity of the residual distribution suggests that caution must be exercised in the ongoing structure analysis, which was also the argument suggested by Le Bail [6]. For this reason, we will limit ourselves to estimate the fraction of the “amorphous” paracrystal in the mixture. In any case we report in Table 1 lattice

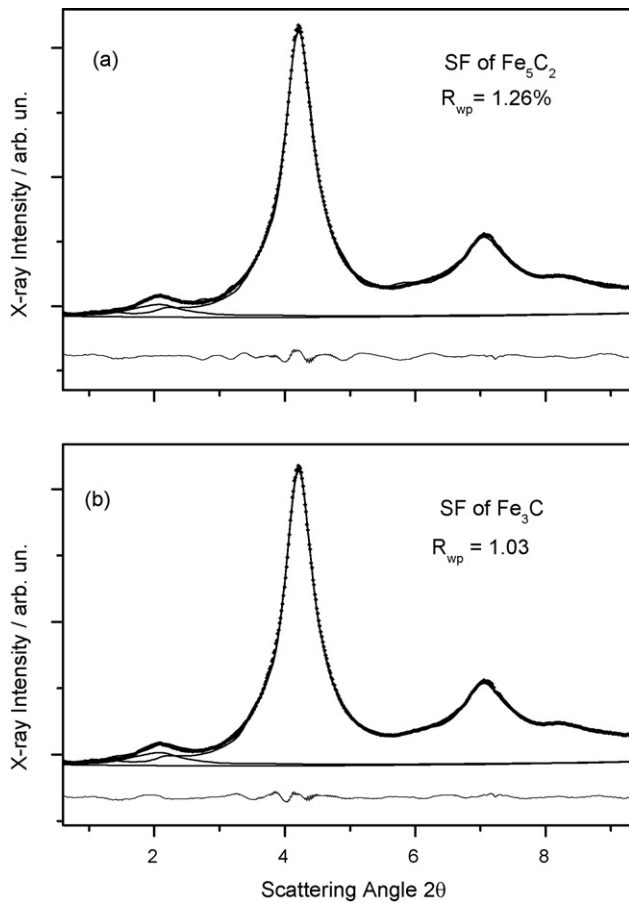


**Fig. 1.** XRD pattern of fully amorphous  $\text{Fe}_{48}\text{Cr}_{15}\text{Mo}_{14}\text{Y}_2\text{C}_{15}\text{B}_6$  bulk metallic glass and corresponding Rietveld refinement. Experimental data (points) and best-fit with a paracrystalline structure factor (full line) are reported for (a) the monoclinic  $\text{Fe}_5\text{C}_2$  (S. G.  $\text{C}_{12}/\text{C}_1$ ) and (b) orthorhombic  $\text{Fe}_3\text{C}$  (S. G.  $\text{Pnma}$ ) type crystal structures. A further paracrystalline model for amorphous silica accounts for capillary glass.

parameters and fractional coordinates of atoms of the “paracrystal” refined at the end of the fit to the intensity profile of the fully amorphous specimen.

On increasing the temperature, several diffraction peaks due to the presence of crystalline phases appeared from the amorphous pattern because of crystallisation. The semi-crystalline Rietveld refinement is now easy to carry out in correspondence of the first crystallisation event, where the formation of  $\text{Cr}_{23}\text{C}_6$ -type phase occurs, because the only matter becomes to introduce the appro-

**Table 1**

“Pseudo cell” lattice parameters and general atomic fractional coordinates (with Wyckoff symbols) of orthorhombic  $\text{Fe}_3\text{C}$  (Space group  $\text{Pnma}$  no. 62) used as a paracrystal to account for the amorphous scattering profile. Special coordinates in bold are fixed by the symmetry conditions. The parameters corresponding to the crystalline unit cell are given in parenthesis. The expansion of the pseudo unit cell of ca 8% accounts for a diminished density in the amorphous structure, at parity of atomic presence, with respect to the crystalline counterpart.

Lattice constants	$a$ (Å)	5.08 (5.09)
	$b$ (Å)	7.32 (6.74)
	$c$ (Å)	4.55 (4.53)
Volume	$V_c$ (Å <sup>3</sup> )	168.5 (155.4)
General atomic positions	Fe (8d)	$x=0.237$ ; $y=0.056$ ; $z=0.344$
	Fe (4c)	$x=0.038$ ; $y=0.25$ ; $z=0.802$
	C (4c)	$x=0.716$ ; $y=0.25$ ; $z=0.260$
Isotropic size	$\langle D \rangle$ (Å)	40
Strain	$\langle e^2 \rangle$	0.04

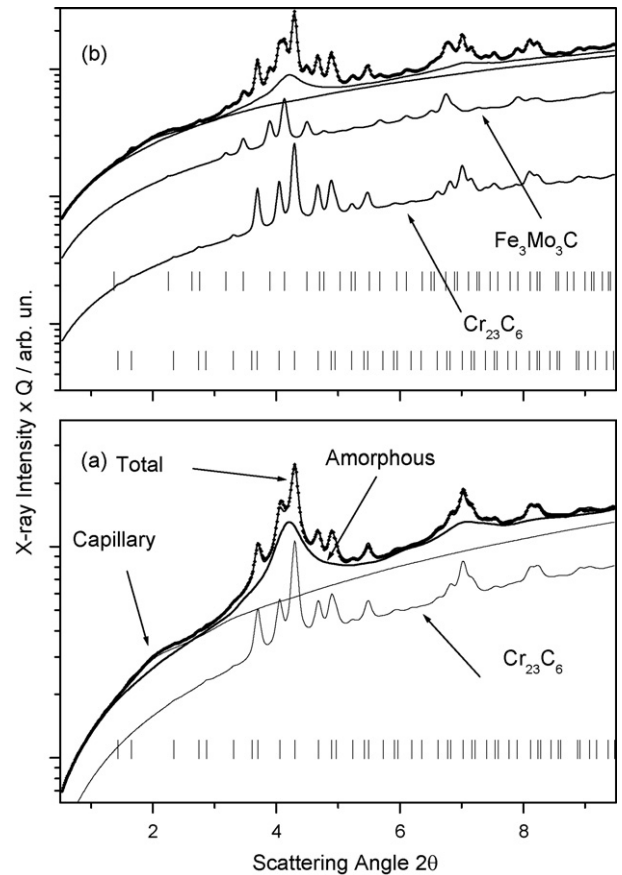


**Fig. 2.** XRD pattern of  $\text{Fe}_{48}\text{Cr}_{15}\text{Mo}_{14}\text{Y}_2\text{C}_{15}\text{B}_6$  bulk metallic glass in correspondence of the (a) first and (b) second crystallisation event and corresponding Rietveld refinement. Experimental data (points) and best-fit making a joint use of the paracrystalline model for the amorphous component and of the  $\text{Cr}_{23}\text{C}_6$ -type and  $\text{Fe}_3\text{Mo}_3\text{C}$ -type structure factor for the Bragg peaks of the precipitated phase (full lines). Data are reported in logarithmic scale. The relevant finger-print sequence of bars is evidenced.

appropriate structure factor of the newly precipitated phase, while keeping fixed the previously optimized parameters of the amorphous components, apart from their volume or weight fraction. This is equivalent to set fixed the composition and “pseudo-structure” of the amorphous phase during the refinement of semi-crystalline pattern. The experimental data (points), and full lines of total fit plus individual curves optimized according to this procedure are shown in Fig. 2a. The contribution of the two amorphous components are shown again above the polynomial background together with the contribution of the  $\text{Cr}_{23}\text{C}_6$ -type phase, which appears displaced of an arbitrary quantity below the background line for the sake of clarity. The sequence of bars at the figure bottom marks the position of each peak expected from the cubic  $Fm3m$  space group symmetry and lattice parameter of the  $\text{Cr}_{23}\text{C}_6$ -type phase.  $\text{Fe}_3\text{Mo}_3\text{C}$ -type phase (space group  $Fd3m$ ) occurred during the second crystallisation process and the simultaneous presence of two crystalline intermetallics with amorphous matrix and silica glass is depicted in Fig. 2b, showing the contribution of each phase. The subsequent step of crystallisation leads to a significant grain refinement and to the disappearance of any contribution from the amorphous metal phase [14,15].

From the Rietveld analysis of diffraction patterns, phase fractions and reliable structure and microstructure average parameters for the crystallised phases have been obtained as a function of temperature (i.e. run number). Neglecting the contribution due to the quartz crucible (i.e., assuming that it makes part of the background), the volume fractions of amorphous (paracrystalline) and

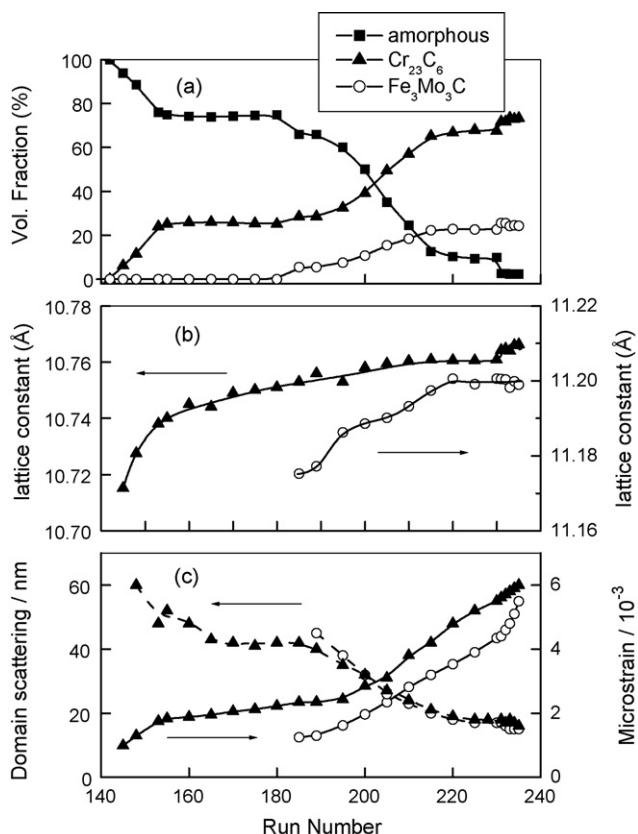


**Fig. 3.** Results of the Rietveld analysis of the crystallisation process in  $\text{Fe}_{48}\text{Cr}_{15}\text{Mo}_{14}\text{Y}_2\text{C}_{15}\text{B}_6$  bulk metallic glass: (a) volume fraction of all phases, (b) lattice parameters, (c) crystal size and microstrain of  $\text{Cr}_{23}\text{C}_6$ -type and  $\text{Fe}_3\text{Mo}_3\text{C}$ -type phases as a function of run number.

**Table 2**

Values of the general fractional coordinates refined by the MAUD program and Wyckoff symbols for the  $\text{Cr}_{23}\text{C}_6$ -type and  $\text{M}_6\text{C}$ -type phases, respectively. In parenthesis the values from single crystal structure solution.

$\text{Cr}_{23}\text{C}_6$ phase		
General atomic positions	Cr (32 f)	$x = y = z = 0.388$ (0.385)
	Cr (48 h)	$x = 0; y = z = 0.185$ (0.185)
	C (24 e)	$x = 0.275$ (0.277); $y = z = 0$
$\text{M}_6\text{C}$ phase (M = Fe, Mo)		
General atomic positions	M1 (Fe) (32 e)	$x = y = z = 0.846$ (0.832)
	M2 (Mo) (48 f)	$x = 0.181$ (0.198); $y = z = 0$

crystal phases have been calculated (Fig. 3a). Increasing the temperature, lattice parameters of crystal phases increased for the thermal expansion (Fig. 3b). The unit cell size can also increase because of the change in the composition. In fact, changes in the occupancy factor in (Fe,Cr) or (C,B) crystal site might change the lattice constant. In a first approximation, we have assumed that the  $\text{M}_{23}\text{C}_6$  is actually  $\text{Cr}_{23}\text{C}_6$ , while the  $\text{M}_6\text{C}$  phase has composition  $\text{Fe}_3\text{Mo}_3\text{C}_{0.5}\text{B}_{0.5}$ . This neglects the contribution from Y atoms and may not reflect the actual composition of phases but it gives a relative evaluation of the vol.% phase changes. The general fractional coordinates of the two cubic phases were refined by the MAUD program. During the thermal treatment they turned out to be substantially unchanged with respect to values of single crystal data reported in the literature. Our refined values are reported in Table 2 for the sake of comparison. Crystal size of both phases increased as the temperature (i.e. run number) increased and, on the other hand, microstrain of both phases reduced (Fig. 3c).

In summary, the crystallisation occurs in three distinct steps. In the first stage, the primary crystallisation of a  $\text{Cr}_{23}\text{C}_6$ -type phase was observed. For increasing temperatures, the eutectic growth of  $\text{Cr}_{23}\text{C}_6$ -type and  $\text{Fe}_3\text{Mo}_3\text{C}$ -type phases was outlined. Finally, the complete disappearance of the amorphous phase and the corresponding growth of the crystalline phases were observed.

#### 4. Discussion

From the example here considered, dealing with amorphous-to-crystalline transformation phenomena induced by the thermal treatment, it emerges that the Rietveld method can be modified with little crystallographic effort and adopted as a self-consistent tool for examining in a quantitative manner a variety of structure situations including the “mixed” condition of semi-crystallinity. A successful application of the present approach demands the availability of a suitable description for the amorphous phase in terms of a structure factor modified according to the view of a paracrystal, as it was proposed by Hosemann and Bagchi [16,4]. Although many examples are known from the literature of semi-crystalline systems, complete structure description of the crystallisation processes starting from a fully amorphous matrix with a global and “coherent” refinement structural approach has been rarely reported. For example, in the case of polymers, the Ruland method [7] gives the integral scattering equation to define the “crystallinity” fraction, but the structure properties of the amorphous matrix needed be separately examined with the radial distribution function method. Other powder diffraction methodologies developed “ad-hoc” are needed for the study of eventually nucleated and crystallised phases. On the other hand, semi-crystalline or nanocrystalline systems have recently been examined with the RDF approach according to Billinge and co-workers [17]. One drawback of the method, which is sensible in the case of a fully amorphous system, is that the total pair distribution function derived from Fourier inversion of the structure factor is scrambled over the possible amorphous and crystalline components. Recognizing the structural terms belonging to the various contributing phase in the real space according to this procedure may be very difficult, especially because the three-dimensional information of a crystalline component becomes lost after projection on a single radial dimension. Thus, only very simple cubic or hexagonal geometries can be recognized, if present, with the Billinge’s approach [17].

Conversely, the method here presented may be applied to all types of systems whether they are single phase, amorphous or multiphase, mixed or polycrystalline. With respect to the classic refinement approach, the only new matter is to access to a structure factor enough flexible according to the paracrystalline conception, to mimic adequately the amorphous profile behaviour. According to Le Bail [6], when a fully amorphous pattern of the system is available, it appears always possible to approximate the amorphous scattering starting with a triclinic paracrystal, structure factor [18]. The efforts here presented show that certain metallic systems, like transition metal–metalloid with composition around 3–1, may actually be described with a more symmetric orthorhombic structure factor. When the paracrystal approach gives close agreement in the diffraction domain, there might be sensible information also on a short-range order that can be accessed from the three-dimensional atomic location in the “pseudo-unit” deformed by the refinement approach. Of course one should be aware of “false” meaningless solution that may occur when using refinement techniques.

#### 5. Conclusions

In this contribution, a “paracrystallinity” approach is proposed in order to ascertain for the best models able to describe an amor-

phous structure with highly distorted lattice that exhibits only very broadened diffraction peaks. In this model, the existence of a “pseudo” unit cell accounts for a pseudo-crystalline structure condition at micro- or nano-scale, with an abnormal amount of lattice strain (ca 2.0%) and extremely reduced coherent diffraction domain size (in our case 4 nm). This analysis has been performed on XRD patterns of fully and partially amorphous BMG by Rietveld refinement using the paracrystal model, although the structure information may not be completely sensible from the physical point of view.

### Acknowledgments

The authors acknowledge financial support by Regione Piemonte (Progetto D23 and Progetto NANOMAT - Docup 2000-2006, Linea 2.4°) and by European Community (Project MCRTN-CT-2003-504692). We thank Prof. G. Cocco and L. Schiffini (University of Sassari) for many helpful discussions concerning the paracrystalline modelling included in the Rietveld refinement.

### References

- [1] P.H. Gaskell, M.C. Eckersley, A.C. Barnes, P. Chieux, *Nature* 350 (1991) 675.
- [2] G. Cocco, S. Enzo, M. Sampoli, L. Schiffini, *J. Non-Cryst. Solids* 61–62 (1984) 577.
- [3] J. Sietsma, B. Thijssse, *J. Non-Cryst. Solids* 101 (1988) 135.
- [4] R. Hosemann, S.N. Bagchi, *Direct Analysis of Diffraction by Matter*, North-Holland, Amsterdam, The Netherlands, 1962.
- [5] R.A. Young (Ed.), *The Rietveld Method*, University Press, Oxford, UK, 1993.
- [6] A. Le Bail, *J. Non-Cryst. Solids* 183 (1995) 39.
- [7] R.L. McGreevy, L. Pustzai, *Molec. Simul.* 1 (1988) 359.
- [8] W. Ruland, *Acta Cryst.* 14 (1961) 1180.
- [9] P. Riello, P. Canton, G. Fagherazzi, *J. Appl. Cryst.* 31 (1998) 78.
- [10] A.G. De La Torre, S. Bruque, M.A.G. Aranda, *J. Appl. Cryst.* 34 (2001) 196.
- [11] L. Lutterotti, R. Ceccato, R. Dal Maschio, E. Pagani, *Mater. Sci. Forum* 278–281 (1998) 93.
- [12] L. Lutterotti, S. Gialanella, *Acta Mater.* 46 (1998) 101.
- [13] A.M. Hindeleh, R. Hosemann, *J. Mater. Sci.* 26 (1991) 5127.
- [14] T.A. Baser, S. Enzo, G. Vaughan, A.R. Yavari, M. Baricco, *J. Mater. Res* 23 (2008) 2166.
- [15] M. Motyka, E. Gilardi, G. Heunen, M. Baricco, *Mater. Trans.* 43 (2002) 1907.
- [16] R. Hosemann, S.N. Bagchi, *Acta Cryst.* 5 (1952) 612.
- [17] M.F. Thorpe, V.A. Levashov, M. Lei, S.J.L. Billinge, *From Semiconductors to Protein: Beyond the Average Structure*, Plenum, New York, USA, 2002.
- [18] C. Cannas, A. Musinu, G. Piccaluga, C. Deidda, F. Serra, M. Bazzoni, S. Enzo, *J. Sol. St. Chem.* 178 (2005) 1526.